International Journal of Heat and Mass Transfer 108 (2017) 2262–2272

Contents lists available at ScienceDirect

International Journal of Heat and Mass Transfer

journal homepage: www.elsevier.com/locate/ijhmt

An improved method of gas well deliquification using supersonic nozzle

Peng Chang *, Bofeng Bai

The State Key Laboratory of Multiphase Flow in Power Engineering, Xi'an Jiaotong University, Xi'an, Shaanxi, China

ARTICLE INFO

Article history:
Received 8 August 2016
Received in revised form 9 January 2017
Accepted 13 January 2017
Available online 31 January 2017

Keywords:
Supersonic nozzle
Liquid atomization
Deliquification
Gas wells

ABSTRACT

Liquid loading from condensed fluids will cause the gas to flow intermittently, sharply reduce the production, which may completely stops. However, the currently existing gas well deliquification technologies are not competitive due to the large volume and extremely high operation expenses. The approach is thus proposed in this paper by establishing the liquid atomization through a supersonic nozzle in high-speed gas environments. The natural-gas condensate and water are therefore pushed into a moving stream of gas where they are broken up into small droplets and flushed away. This approach is especially suited for low-pressure and low-yielding wells. Numerical and experimental studies are firstly performed to determine the optimal nozzle structure. The exit velocity can reach 5–6 times the speed of sound. As expected, the magnitude of the gas velocity determines the droplet size, which ranges from 10 μm to 50 μm in most circumstances and is far less than the minimum threshold for being discharged. A year-long field test on three producing gas wells is conducted to validate the applicability of this method, the water and condensates build-up are removed completely to maintain the long-term stability and productivity in gas production. Also, this method enables to extend the useful life of equipment, reduce downtime and maximize the production capabilities.

1. Introduction

Liquid loading is the inability of a producing gas well to remove liquids that are produced from wellbores [1]. Dousi et al. [2] constructed a model to enhance the understanding of the process of liquids build up in gas wells. As gas wells mature, a lower production velocity is caused as production volumes and bottom-hole pressure begin to decrease, and the liquids cannot be carried to the surface. The produced liquids then accumulate at the bottom of the wellbore, create more back pressure against formation pressure, and sharply decrease the gas production. The wells may eventually die if the liquids are not continuously removed [3]. The technologies for addressing this problem continue to advance [4]. Researches and developments are constantly being performed to make these deliquification methods more effective. The commonly used solutions include foam treatment, velocity strings, plunger lift, vortex tool, evaporation, electric submersible pumps, compression, hydraulic pumping, downhole atomization, etc. [5–12]

Downhole atomization is an improved method for removing liquids from wellbores so as to reduce the hydro static head, unload the wells and permit more efficient production of gas [12–14]. Li et al. [15] theoretically investigated a new technological method to utilize a downhole atomized nozzle changing the borehole gas-liquid two-phase flow into the mist flow. Harris et al. [16] developed an artificial lift system for deliquification of gas production wells, which comprises a downhole tool suspended by a power conductive cable in a wellbore. The downhole tool includes an atomizing chamber for conversion of the liquid into droplets having an average diameter less than or equal to 10,000 μm. Levitan et al. [17] proposed a method to increase the production of a hydrocarbon wellbore at its medium and last stage of exploitation. The device includes a mandrel and sealing assembly with a nozzle installed inside the mandrel and above the sealing assembly, creating a low pressure zone in the tubing of the well and evacuating the liquid phase. Most of the existing atomization methods are established through a narrow orifice and the average diameter of liquid droplets generated is relatively large. Moreover, the optimum method used to deliquify gas wells should be defined as that is most economic for the longest period of operation. Nevertheless, according to our experience, these existing methods are energy intensive and labor-intensive. The convergence of large volume, vendor equipment availability, and high operating costs make them inconvenient and impractical to utilize. Detailed comparison can be found in Table 2.

In addition, attaining a full understanding about flow regimes in gas wells is very important. Visible in past experimental and

* Corresponding author.
E-mail addresses: camerfish@stu.xjtu.edu.cn (P. Chang), cpyanzi@163.com (B. Bai).

http://dx.doi.org/10.1016/j.ijheatmasstransfer.2017.01.054
0017-9310/

Nomenclature

x	axial distance along fluid flow axis, m
y	gap-wise direction, m
u	fluid velocity vector, m/s
v	fluid velocity vector, m/s
P	pressure, Pa
T	temperature, K
d	diameter, m
A	surface area, m^2
k	turbulent kinetic energy, J/kg
G	Gravity, N
Ma	Mach number
C_p	Heat capacity, J/(kg K)

Greek symbols

ρ	density, kg/m^3
ξ	friction factor
κ	thermal conductivity, W/(m K)
γ	specific heat ratio
ε	turbulent dissipation, J/kg s
ω	specific rate of dissipation, 1/s

Subscripts

l	liquid
g	gas
avg	average

numerical studies, there are four flow patterns commonly seen in vertical and sharply inclined pipes, which are often separated from each other by transition regions [18]: bubbly flow, slug flow, churn flow, annular flow and dispersed bubble. During the progression of a typical gas well from initial production to end of life, it may go through any or all of these flow regimes. The flow at the surface maintains mist flow until the conditions change sufficiently at the surface to force the emergence of the transition flow. At this point, the well production becomes erratic and the flow progresses to slug flow, which is often be accompanied by a marked increase in the declined gas production rate. As the gas rate further decreases, liquids cannot be carried to the surface and a stagnant liquid column is formed thereby. If no corrective action is taken, the well may eventually log off.

The interest stemming from the possibility of overcoming the barriers mentioned above, this paper develops an economic method to deliquify gas wells by using a supersonic nozzle to atomize liquid. At the high-speed environment, a supersonic gas jet can be produced at the moment of impact and injected into the liquid storage section, and then, penetrates further away from the nozzle exit. By the virtue of the shear forces generated by the gas jet and the subsequent pressure gradient, the continuous liquid film thins and eventually breaks into small droplets, becoming the dispersed phase.

The consideration in selecting the optimum supersonic configuration includes economic factors, production scales, physical properties of the fluid to be atomized and the droplets to be produced, and the morphology of the droplets desired. Firstly, numerical studies and experimental verifications are performed to determine the nozzle configuration, which has the best atomization efficiency and can generate the smallest drops under a wide range of scenarios. After the experimental results and the model predictions closely correspond, a year-long field test on three producing gas wells is done to practically testify this deliquifying technique. Unlike traditional methods, this method presents numerous distinct advantages applying to dewatering gas wells as well as typical production installations, such as simple and compact, highly reliable, low-cost and low-risk to operate, high efficiency, and no requirements for auxiliary equipment, which make it to be potentially competitive for the long period of operation.

2. Methodology

The mist flow regime normally requires relatively high gas flow rates, which means if a gas well is flowing gas at a rate greater than the critical rate, the gas velocity is sufficient to carry liquids as a fine mist or small droplets to the wellbore surface. However, in flowing gas wells, where the gas velocity is unable to lift the liquid from the bottom of the wellbore to the surface, the liquids fall back and accumulate in the bottom of the tubing. It is generally believed that the liquids are both lifted in the gas flow as individual particles and transported as a liquid film along the tubing wall by the shear stress at the interface between the gas and the liquid before the onset of severe liquid loading. These mechanisms were first investigated by Turner et al. [19], who discovered that liquid loading could best be predicted by the droplet model when droplets moved up (gas flow above the critical velocity) or down (gas flow below the critical velocity). There are three forces applied to the liquid droplet, namely, gravity, drag force and buoyancy.

The droplet weight acting downward is given by,

$$G = \pi/6 d^3 \rho_l \tag{1}$$

The buoyancy acting upward can be expressed as,

$$F = \pi/6 d^3 \rho_g \tag{2}$$

where G is the gravity (N); d is the droplet diameter (m); F is the buoyancy (N); ρ_l and ρ_g are the density of liquid and gas, respectively (kg/m^3). The drag force from the gas acting upward is expressed by the drag equation, which is used to calculate the force of drag experienced by an object due to movement through a fully enclosing fluid.

$$R = \xi\pi/4 d^2 \rho_g g u^2/2g \tag{3}$$

Here, R is the drag force (N); ξ is the friction factor, u is the fluid velocity (m/s) and g is the gravitational constant (m/s^2). When the three forces are in equilibrium, the gas velocity is at "critical" and can be calculated by,

$$u = \left[\frac{4gd(\rho_l - \rho_g)}{3\xi\rho_g}\right]^{0.5} \tag{4}$$

Eq. (5) predicts the minimum critical droplet diameter required to transport the liquids in a vertical well bore,

$$d < \frac{3u^2\xi\rho_g}{4g(\rho_l - \rho_g)} \tag{5}$$

Having the critical diameter $\left(d_{cri} = \frac{3u^2\xi\rho_g}{4g(\rho_l-\rho_g)}\right)$, the droplets would be suspended in the gas stream, moving neither upward nor downward. If the droplet diameter $d > d_{cri}$, the droplets fall and liquids accumulate in the wellbore; if $d < d_{cri}$, the liquids can be removed and the gas wells are prevented from loading with liquids. Accord-

ing to the known daily gas production of 997.3 m^3/d and 4989.33 m^3/d, and the casing pressure of 3.5×10^6 Pa, the calculated d_{cri} is 0.05 mm and 0.5 mm, respectively.

Several works have been done to investigate the drop size distribution in terms of related parameters [20–23]. Generally accepted findings are the drop size decreases with increasing gas velocity. In this study, the supersonic atomizer is placed in the liquid storage zone. By employing a converging-diverging nozzle, the supersonic jets are developed and complex interactions of reflection and diffraction appear inside the nozzle. High-speed convective flow plays a dominant role in the breakup process and Mach number (Ma) being 6.8 can be reached.

For the steady isentropic flow with changing cross-sectional area,

$$\frac{A}{A_*} = \frac{1}{Ma} = \left(\frac{1 + \frac{\gamma-1}{2}Ma^2}{\frac{\gamma+1}{2}}\right)^{\frac{\gamma+1}{2(\gamma-1)}} \tag{6}$$

where A is the cross-sectional area (m^2) and γ is the specific heat ratio.

Additionally, the velocity with area change for 1D isentropic flow is calculated as,

$$\frac{du}{u} = -\frac{1}{Ma^2 - 1}\frac{dA}{A} \tag{7}$$

As depicted in Fig. 1, the speed of the subsonic flow of gas increases in the converging section. At the throat, where the cross-sectional area is minimum, the gas velocity locally becomes sonic (Ma = 1.0). In the diverging section, the gas begins to expand and the gas flow increases to supersonic velocities where a sound wave will not propagate backwards through the gas.

3. Simulation

According to our preliminary experiments, it is found that the smaller droplet size and size distribution range of breakup droplets can be obtained at higher velocities, which result in the better liquid displacement efficiency. The numerical study is required to design and improve the nozzle structure. Due to the complexity of the atomizer simulations, the formation of liquid droplets is not considered here.

There are several governing equations associated with converging-diverging nozzles that are taken into considerations in theoretical calculations and form the fundamentals of majority of computational fluid dynamics software such as ANSYS FLUENT, which has been applied in this work [24]. The continuity equation (Eq. (8)), Navier-Stokes equations (Eqs. (9) and (10)) along with the energy equation (Eq. (11)) are solved simultaneously.

$$\frac{\partial \rho}{\partial t} + \frac{\partial(\rho u)}{\partial x} + \frac{\partial(\rho v)}{\partial y} = 0 \tag{8}$$

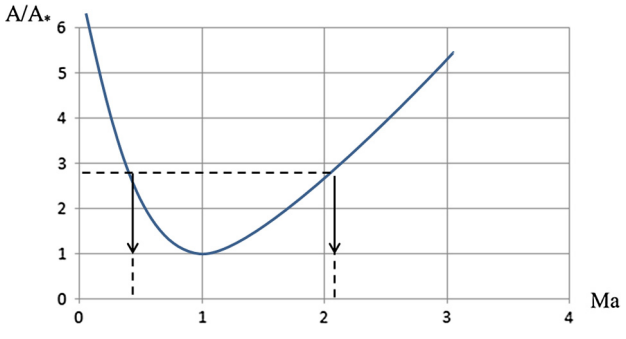

Fig. 1. The area ratio versus *Ma*.

$$\rho\left(\frac{\partial u}{\partial t} + u\frac{\partial u}{\partial x} + v\frac{\partial u}{\partial y}\right) = -\frac{\partial p}{\partial x} \tag{9}$$

$$\rho\left(\frac{\partial v}{\partial t} + u\frac{\partial v}{\partial x} + v\frac{\partial v}{\partial y}\right) = -\frac{\partial p}{\partial y} \tag{10}$$

$$\rho C_p\left(\frac{\partial T}{\partial t} + u\frac{\partial T}{\partial x} + v\frac{\partial T}{\partial y}\right) = \frac{\partial}{\partial x}\left(\kappa\frac{\partial T}{\partial x}\right) + \frac{\partial}{\partial y}\left(\kappa\frac{\partial T}{\partial y}\right) \tag{11}$$

where u and v are the velocity vectors in Cartesian Coordinates (m/s), p is the pressure (Pa); T is the temperature (K) and κ is the thermal conductivity (W/m K). There are two most typical turbulence models used in the simulations, k-ε model & k-ω model. k is the turbulent kinetic energy (J/kg), ε is the turbulent dissipation (J/kg s), and ω is the specific rate of dissipation (1/s). Sometimes, these two models have sizeable numerical differences. In most cases the difference is in convergence time and the number of iterations. k–ε model is more feasible for fully turbulent flows. The model performs poorly for complex flows involving high pressure gradient, separation, and strong streamline curvature. The most significant weakness is lack of sensitivity to adverse pressure gradients. Basically, this model is suitable for initial iterations, initial screening of alternative designs, and parametric studies. k-ω model allows for a more accurate near wall treatment with an automatic switch from a wall function to a low-Reynolds number formulation based on grid spacing. It performs significantly better for complex boundary layer flows under adverse pressure gradient conditions. Due to the aforementioned advantages, k-ω model is chosen for this study.

A series of simulations are conducted on the nozzle geometry available in Fig. 2 with flow conditions corresponding to an injection pressure of 5 Mpa, a background pressure of 0.35 Mpa, and an ambient temperature of 27 °C. Gas compressible flow is assumed through the axisymmetric converging-diverging nozzle and only a two dimensional portion is simulated. Here, we only present the results of the two typical cases.

For case1, the inlet radius is 2.5 mm, the throat radius is 0.5 mm, and the outlet radius is 4 mm. The axial distance from the inlet to the throat is 12.5 mm and the axial distance from the throat to the outlet is 12.5 mm as well. In the nozzle, the wall-resolved approach is utilized with Δx^+, $\Delta y^+ \sim 1$ near the wall, Δx^+, $\Delta y^+ \sim 20$ near the center. Δx^+, Δy^+ are the non-dimensional wall distances for the wall bounded flow. A mesh of 2 million hexahedral control volumes is used to discretize the computational domain. According to the grid sensitivity study, it is necessary to have the mesh-independent results and optimize the computational time. Mesh points are concentrated in the throat. The numerical boundary conditions are a slip condition over the radial boundaries and a uniform outflow.

The contour of *Ma* and the variation of the axial *Ma* plotted along the centerline are shown in Figs. 3 and 4. The high-pressure low-velocity gas flows through the convergent section in the subsonic condition and contracts in the throat. Then the low-pressure high-velocity gas expands in the divergent section in the supersonic condition.

Manipulating the determinative variables such as the area ratio and the back pressure to regulate *Ma* at the nozzle end can help to locate the optimal design. Another case with the inlet/outlet radius of 3.5 mm, the throat radius of 0.5 mm, the inlet pressure of 5 Mpa, the back pressure of 0.36 Mpa and the operating temperature of 27 °C is investigated. Fig. 5 represents the contour of *Ma*. Due to the increase in volume after the throat in the diverging area, the gas density drops down, causing the velocity to augment and reach the supersonic speed. For this case, the maximum *Ma* is 6.52.

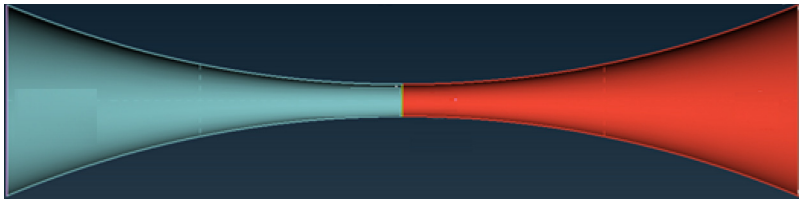

Fig. 2. Schematic of the configured converging-diverging nozzle.

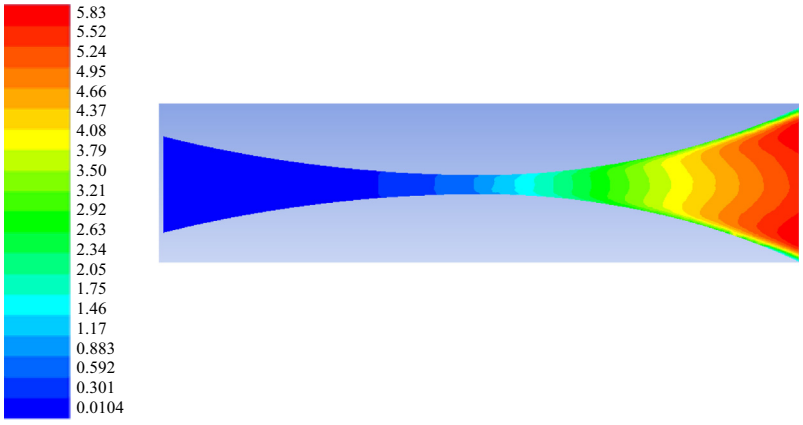

Fig. 3. Contour of *Ma*; the maximum value is 5.83.

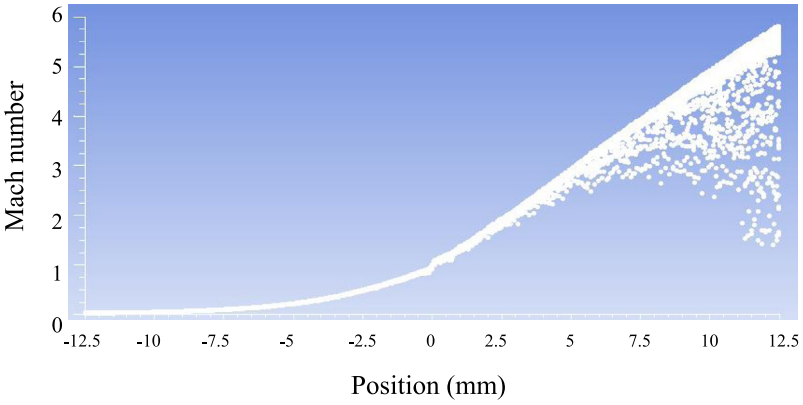

Fig. 4. The variation of the axial *Ma*.

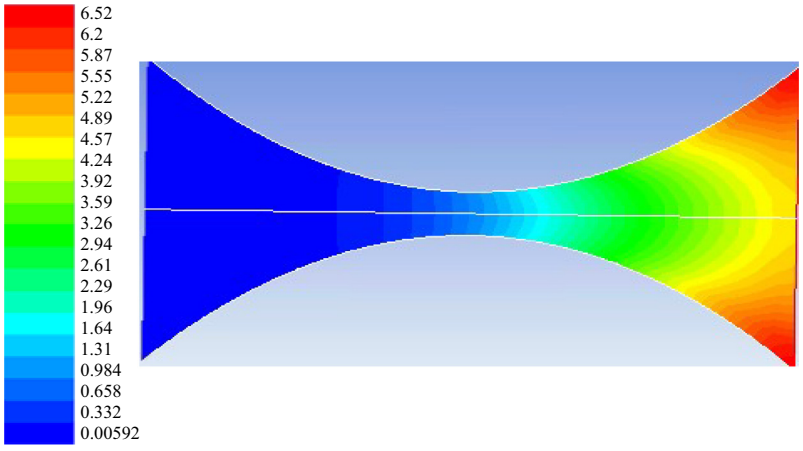

Fig. 5. Contour of *Ma*; the maximum value is 6.52.

4. Experiment validation

Based on the numerical analyses of the nozzle flow, the converging-diverging nozzle with the inlet/outlet radius of 3.5 mm, the throat radius of 0.5 mm is adopted for the subsequent experimental studies to obtain the droplet size distribution.

4.1. Tested nozzles and rigs

The actual operating conditions in Changqing Sugeli oil-field corresponding to the throat diameter of 1–2 mm, the daily gas production of 2500–3500 m^3, and the daily liquid production of 0.15–0.25 m^3 are used as references. In the low-yielding gas wells, it is very difficult to remove liquid droplets entrained in a gas stream. The gas kinetic energy needs to exceed the minimum value to lift the liquids, which makes the nozzle design even more difficult. The experiments are performed on the Oil & Gas & Water test rig in State Key Laboratory of Multiphase Flow in Power Engineering. Fig. 6 gives the schematic arrangement of the experimental apparatus.

The experimental installation for investigating liquid atomization and parameters of the two-phase gas-droplet flow (Figs. 6 and 7) comprises the following main elements: atomizer with spraying device; high-pressure gas supply system; instruments for monitoring and controlling the pressure and flow rate; test section with the systems of optical diagnostics and video and photo recording of the two-phase flow; and system of computerized control of the installation, acquisition and processing of experimental data.

Tests are carried out to atomize liquid at the gas injection temperature of 27 °C. The gas is preliminarily compressed by a high pressure compressor and delivered through a ball valve. The liquid is controlled by a back-pressure valve and a control valve to avoid the reverse flow. The steady-state criterion establishes that, over an uninterrupted 1 h interval, the variation of the temperature readings should be less than 1 °C and the variation of the measured compressor power should be less than 1%. An error propagation analysis yields uncertainties of ±4% for the coefficient of performance. Repeatability tests confirm that the dispersion of the data with respect to the normal distribution was small, with deviations less than 3.5% of the average values.

4.2. Drop diameter measurement and data analysis

Malven Spraytec laser diffraction system allows measurement of spray particle and spray droplet size distributions in real time with accuracy. Its accuracy is checked with a standard reticle. The suggested calibration using the reticle estimates that the measurement uncertainties of spatially averaged Sauter Mean Diameters (SMD or D[3 2]) and Volume Mean Diameter (VMD or D[4 3]) range within ±3%. D[3 2] is the diameter of a drop having the same volume/surface area ratio as the entire spray, it is most sensitive to the presence of fine particulates in the size distribution; While D[4 3] refers to the mean diameter over volume, it is most

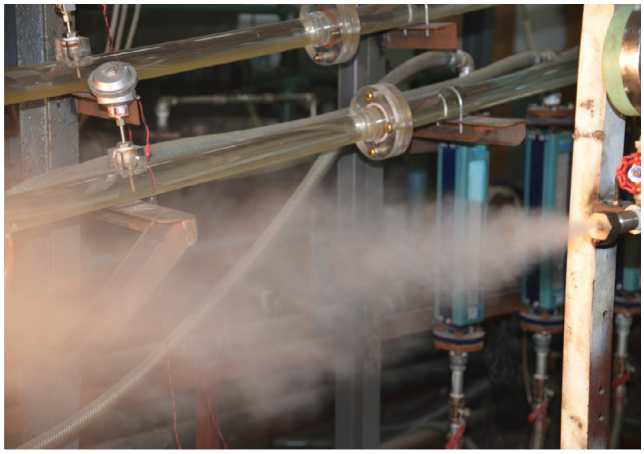

Fig. 7. Spray droplet size measurement.

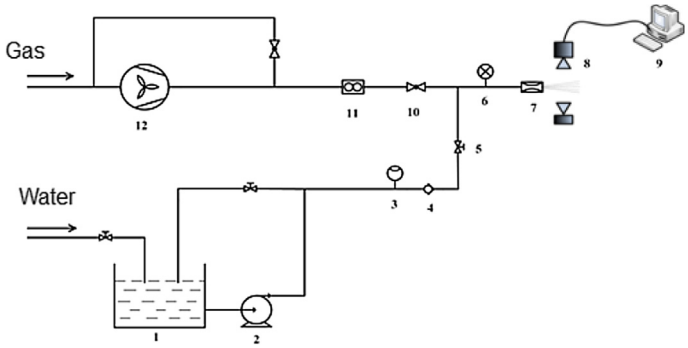

1-Tank 2- Pump 3-Meter 4-Back-pressure Valve 5-Control Valve 6-Pressure Gauge 7-Test Section 8- Spraytec 9-Computer 10-Ball Valve 11- Orifice flowmeter 12-Compressor

Fig. 6. Schematic of experimental apparatus.

Table 1
Summary of experimental parameters.

Condition	Injection pressure (MPa)	Back pressure (MPa)	Gas flow rate (m^3/day)	Liquid flow rate (kg/d)
1	0.5	0.1	2602	266.4
2	0.4	0.1	2046.6	223.2
3	0.3	0.1	1359.97	187.2

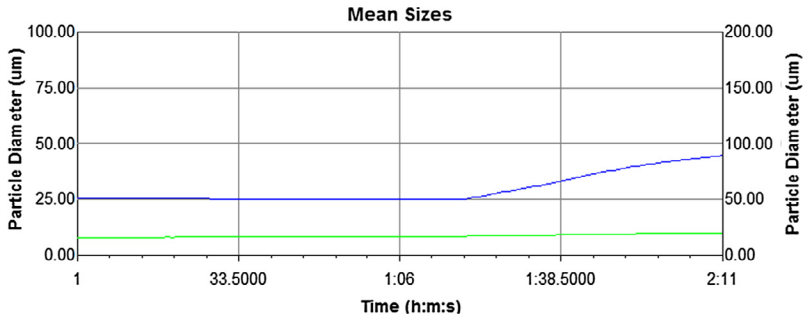

Fig. 8. The mean diameters versus time periods for condition1.

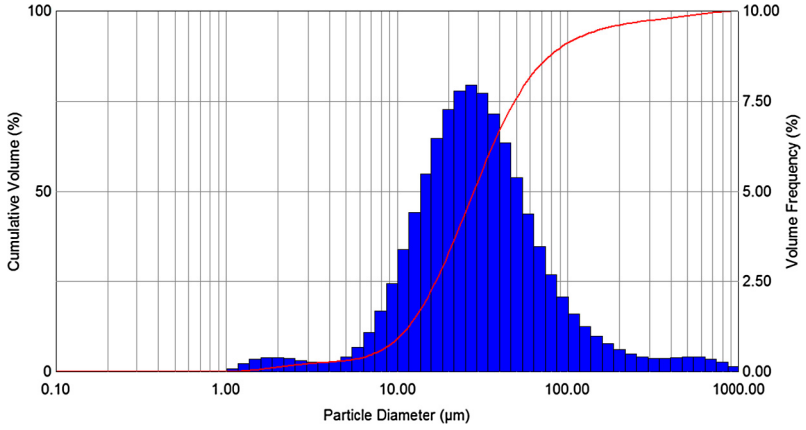

Fig. 9. Spatial-averaged volume-weighted drop size distribution for condition1.

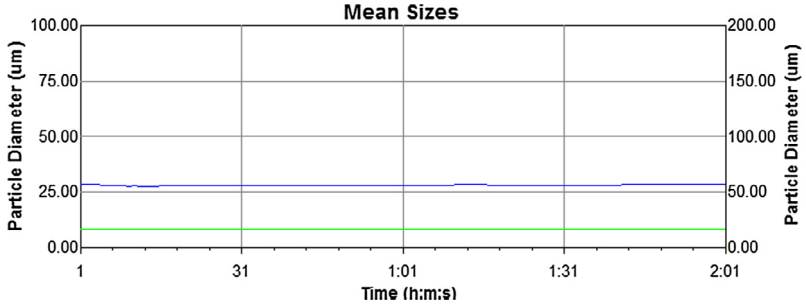

Fig. 10. The mean diameters versus time periods for condition2.

sensitive to the presence of large particulates in the size distribution.

The radially resolved D[3 2] and D[4 3] are expected to have somewhat larger uncertainties, since the tomographic reconstruction induces additional mathematical and numerical uncertainties. Other factors that can contribute to the uncertainty include the drop asphericity, beam steering by the gas jets and non-perfect correction of multiple scattering [25]. The overall uncertainties of D[3 2] and D[4 3] measurements are estimated within ±6%.

4.3. Results and discussion

Table 1 lists all the experimental conditions. The sampling frequency is 1 s with a time interval of 2 min. D[3 2] and D[4 3] are measured in three different scenarios.

Fig. 8 illustrates the mean diameter measured at the specified time-interval. The green[1] solid line represents D[3 2] with an aver-

[1] For interpretation of color in Fig. 8, the reader is referred to the web version of this article.

age value of 18.89 μm, and D[4 3] are denoted by the blue line. The averaged value of D[4 3] is 69.88 μm. The relatively smooth curve is clearly good indicating the stability of the atomization. Spatial-averaged volume-weighted drop size distribution is presented in Fig. 9, which indicates a peak around D[4 3] = 40 μm. The cumulative volume implies that the value for percent less than 40 μm is reported as 65%.

Fig. 10 illustrates that D[3 2] and D[4 3] do not change appreciably with time under condition2, indicating a stable liquid atomization. $D[3\ 2]_{avg}$ = 17.26 μm and $D[4\ 3]_{avg}$ = 56.99 μm. The corresponding particle size distribution data in terms of the cumulative volume frequency is plotted in Fig. 11. There are a large number of droplets with the diameters dropping in the range of 20–40 μm and the droplets smaller than 150 μm are more prone to be captured. In examining Fig. 11, it is interesting to notice a small volume frequency bell curve in the range of 300–1000 μm, indicating that some large drops follow the trajectory of the gas flow. Although not much, their existence augments the D[4 3] measurements.

Fig. 12 shows that the atomization remains stable for conditions3. $D[3\ 2]_{avg}$ = 33.8 μm and $D[4\ 3]_{avg}$ = 105.9 μm. The example of the cumulative frequency plot for distribution that is normally distributed in volume is given in Fig. 13. The sizes of a large portion of drops (70%) are less than 100 μm.

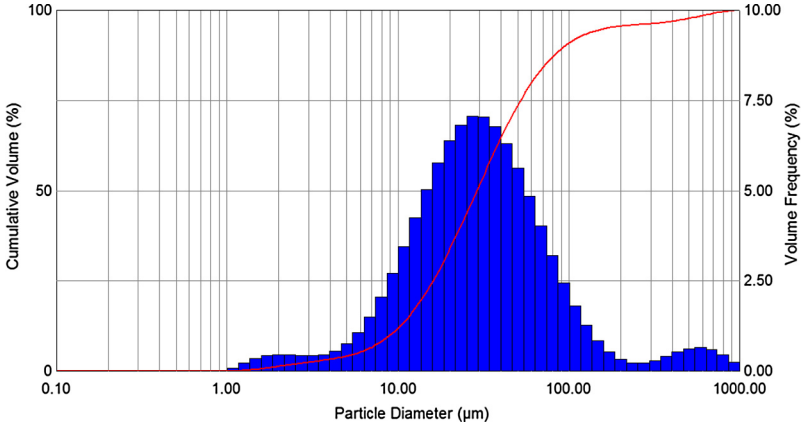

Fig. 11. Spatial-averaged volume-weighted drop size distribution for condition2.

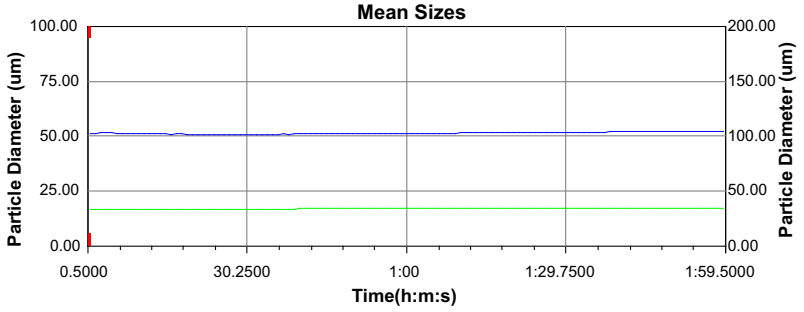

Fig. 12. The mean diameters versus time periods for condition3.

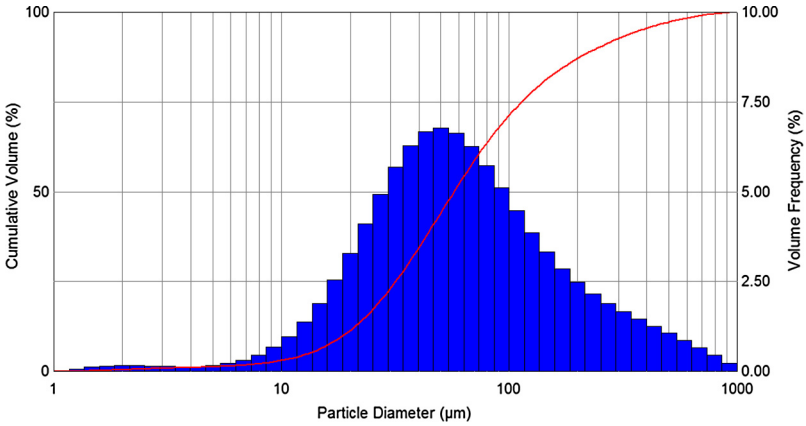

Fig. 13. Spatial-averaged volume-weighted drop size distribution for condition3.

5. Field test

Significant field tests have been related to the evaluation of the response of different gas wells to deliquification using this method since 2013, which is proved to be effective in operating these gas wells more efficiently by reducing the detrimental effects of liquid loading on gas production. The customized atomizing nozzles were mounted in 3 gas wells. Fig. 14 gives the process flow diagram about how the device works inside the gas wells. Before entering into the nozzle, the flow is bubble flow. Gas droplets are carried by the liquid phase and move upwards. When they flow through the convergent section in the subsonic condition, the gas droplets coalescence and push the liquid into the throat. Then, the mixture expands in the divergent section in the supersonic conditions and the liquid is broken up into small droplets and flushed away. The installation position the atomizer is placed in the liquid storage zone at the bottom of the wellbores, slightly over the liquid surface. If the nozzle is installed below the liquid surface, no atomization can be generated; if the installation position is too high, the liquids will accumulate in the wellbores and lower the efficiency of deliquification.

The shape of the well's decline curves is an important indication of downhole liquid loading problems, which should be analyzed for long periods, looking for changes in the general trend. The smooth exponential type decline curve is characteristic of normal gas-only production considering reservoir depletion. The sharply fluctuating curve is indicative of liquid loading in the wellbores and in this case is showing the wells to deplete much earlier than reservoir considerations alone would indicate. Fig. 15 gives the gas production change with time for the three gas wells. During the one-year period, most of the liquids are removed and the flowing tubing pressure at the formation face together with the gas production rate reaches a relatively stable equilibrium.

If the liquids start to accumulate in the bottom of the wellbore, the added pressure head on formation will lower the surface tubing pressure. As the liquid production increases, the added liquid increases the gradient in the tubing and provides more back pressure against the formation and reduce the surface tubing pressure. Furthermore, the presence of liquids is shown as an increase in the surface casing pressure as the fluids bring the reservoir to a lower flow, higher pressure production point. As gas is produced from the reservoir, gas percolates into the tubing casing annulus, which is exposed to the higher formation pressure and causes an increase in the surface casing pressure. Therefore, a decrease in tubing pressure and a corresponding increase in casing pressure are indicators of liquid loading.

In Fig. 15(a), the initial wellhead productive capability of gas well #1 is 1.5×10^4 m^3/day. The instability in the casing/tubing pressures leads to the sharply fluctuating gas production rate, indicating that the well is currently experiencing liquid loading. The atomizing nozzle was installed on Sep. 21st, 2014 and the depth of the installation is 2136 m. At that time, the wellhead productive capability of gas well #1 was 1×10^4 m^3/day due to reservoir depletion. After the installation, the casing pressure drops gradually at the rate of 0.012 Mpa/day indicating no liquid loading in the wellbore.

In Fig. 15(b), the initial wellhead productive capability of gas well #2 is 0.8×10^4 m^3/day. After using the atomizing nozzle on Nov. 12nd, 2014, the wellhead productive capability of gas well #2 is 1.2×10^4 m^3/day and the steady decline of the casing pressure at the rate of 0.012 Mpa/day demonstrates that this approach helps to maintain the stable gas production rate for low-pressure (~5 Mpa) wells. The depth of the installation is also 2136 m. In Fig. 15(c), the initial wellhead productive capability of gas well #3 is 2.8×10^4 m^3/day. The atomizing nozzle was mounted on Aug. 29th, 2014 and the depth of the installation is 2000 m. There is also no obvious tubing pressure drop caused by the accumulated liquids and the gas well is producing at a steady rate.

In addition, flowing or static well pressure surveys are the most accurate methods to determine whether a gas well is loading with liquids or not [26]. Pressure surveys measure the pressure with depth of the well. The measured pressure gradient is a direct function of the density of medium and the depth, and for a single static fluid, the pressure with respect to the depth should be nearly linear. Since the density of the gas is significantly lower than that of the liquid, the measured gradient curve exhibits a sharp change of slope when there is standing liquid in the tubing. Fig. 16 illustrates the measured pressure distribution in a producing gas well. The gas and liquid production rates change the slopes, and the presence of liquids results in the high pressure gradient (0.0025 Mpa/m from 500 m to 1900 m) in Fig. 16(a). After installing the nozzle, the pressure gradient drops to 0.00023 Mpa/m, showing that liquid loading is successfully mitigated.

There are numerous advantages to this method, i.e. applicability over a wide range of well conditions such as low-yielding wells, cost effective (low set-up and low operating costs), versatility for

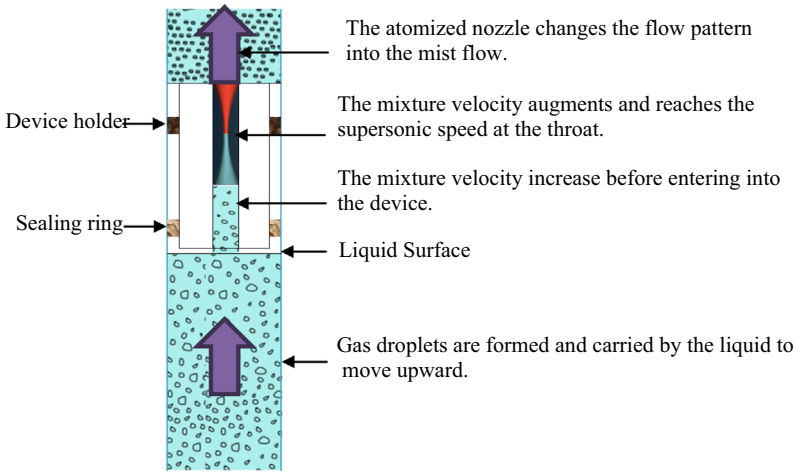

Fig. 14. Process flow diagram of the nozzle installed in gas wells.

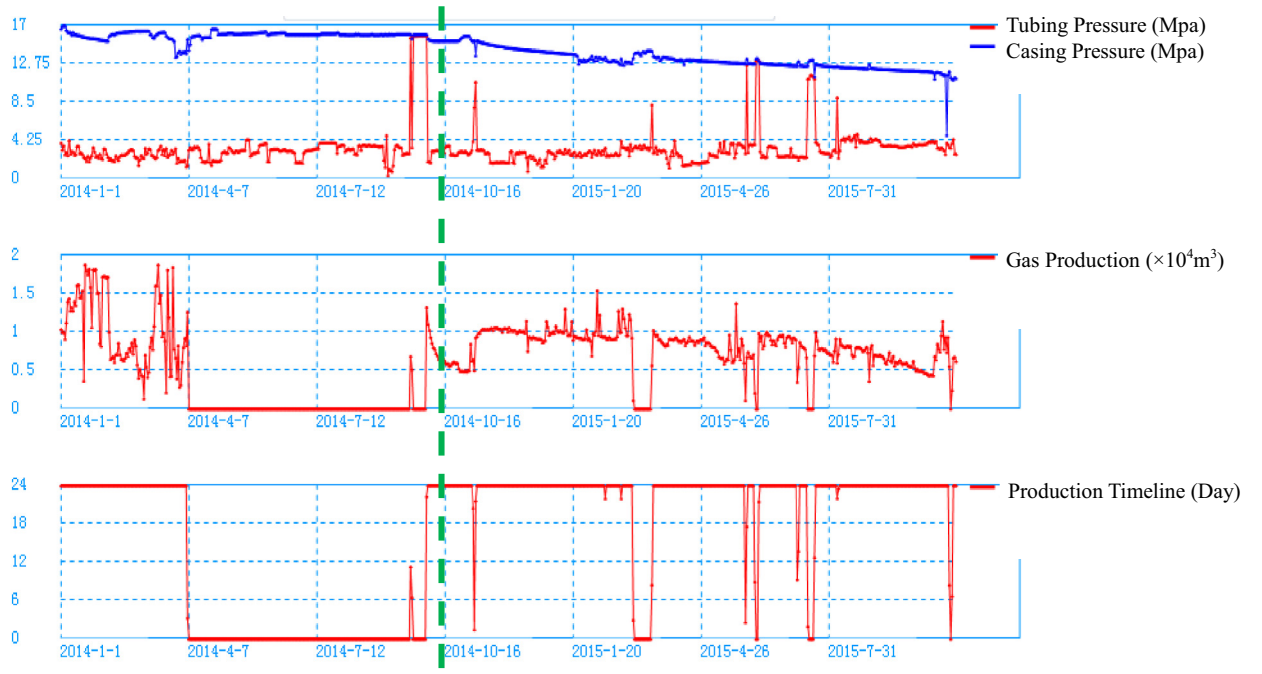

(a) Gas well #1 (Device Installation Date: 2014-09-21)

(b) Gas well #2 (Device Installation Date: 2014-11-12)

Fig. 15. Pressure, gas production rate and time line in three producing gas wells.

different completions and environments, rapid response from the well, no auxiliary equipment needed, etc. It is making gains in deliquification efficiencies and has been proved to be one of the optimum deliquifying methods. Table 2 compares different deliquification techniques that were used or are currently being used by Changqing Sugeli oil-field. As tabulated below, this deliquifying method only costs about 30,000 RMB upon installation and no maintenance is needed for 2–3 years, which is more cost-effective and labor-effective as compared to the other techniques, i.e. foam treatment, coiled tubing, velocity strings and plunger lift.

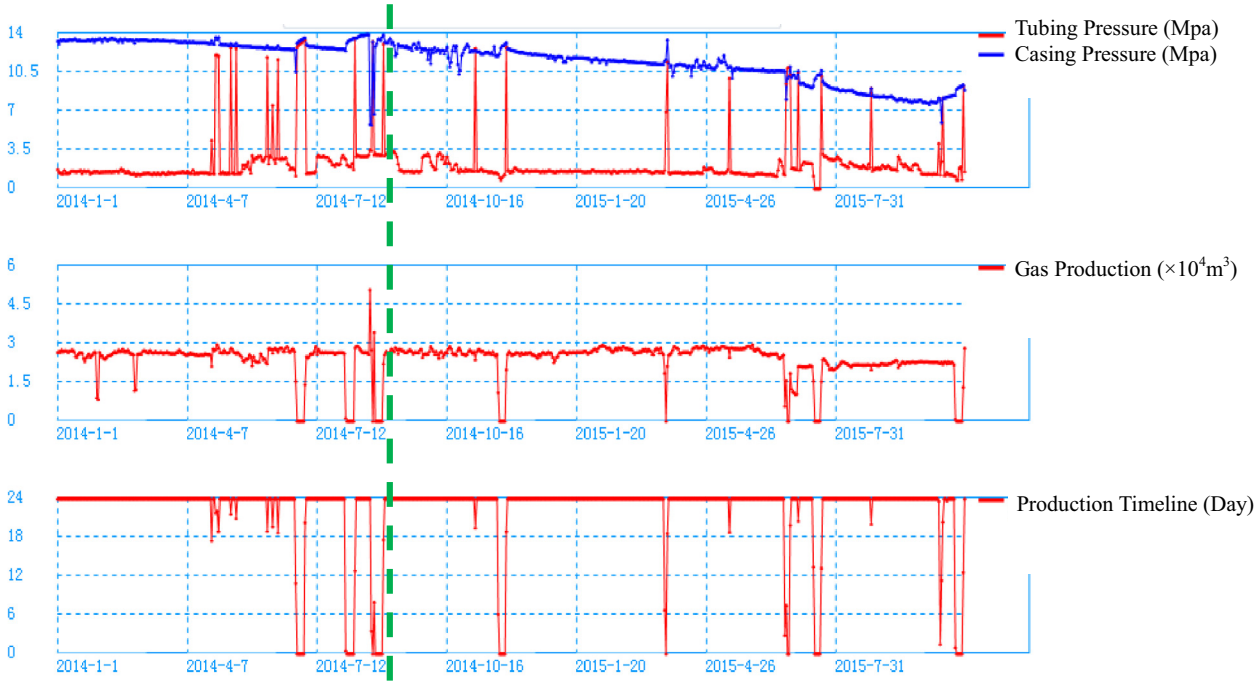

(c) Gas well #3 (Device Installation Date: 2014-08-29)

Fig. 15 (*continued*)

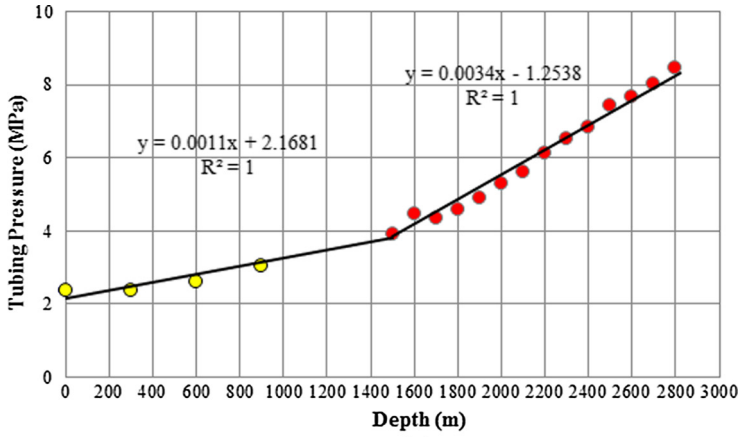

(a)

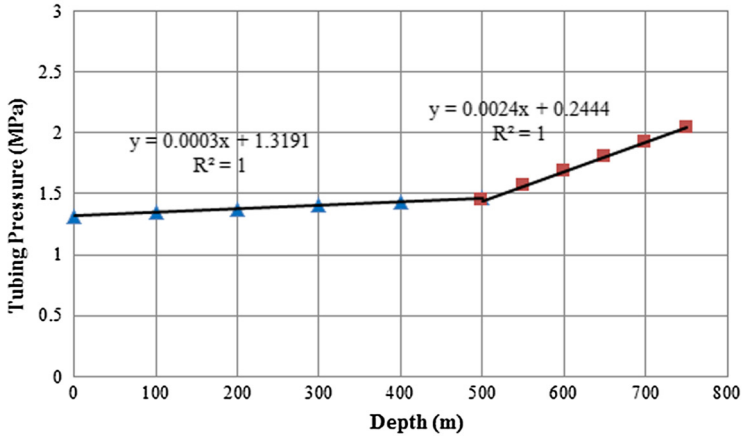

(b)

Fig. 16. Pressure distribution in a producing gas well (a) before and (b) after installing the optimized atomizer.

Table 2
Comparison of different deliquification methods used in changqing sugeli oil-field.

Deliquification method	Cost (RMB)	Usage
Foam treatment	50,000	High labor costs
Coiled tubing Velocity strings	400,000 (3–5 years)	High set-up costs
Plunger lift	180,000 (3–5 years)	High machinery costs
Liquid atomization	30,000	Maintenance-free for 2–3 years

6. Conclusion

For the gas production process to occur, liquid must be removed from the wellbore to prevent the costly losses in gas production. The economic deliquifying method to facilitate the removal of liquids from gas wells is therefore proposed and validated through numerical analysis, experimental investigations and field tests.

1. The liquid atomization through the supersonic nozzle is incorporated into deliquification. The supersonic gas jet produced into the liquid section breaks the liquid film into small droplets, which can then be removed from the wellbores.
2. The exit stream velocity can reach 5–6 times the speed of sound in the optimal configured nozzle. The magnitude of the gas velocity determines the droplet size. As expected, the droplet size lies within the range of 10–50 μm, which is far less than d_{cri}.
3. The one-year field test to evaluate the response of the three gas wells experiencing liquid loading summarizes that the installed nozzles can help to produce gas efficiently and prevent the gas wells from declining and eventually logging off.
4. Proper equipment installation is very important. The nozzle needs to be mounted in the liquid storage zone at the bottom of the wellbores, slightly over the liquid surface.
5. For gas wells having the same production rate, the nozzle structure is determined by the amount of liquids. The compressible area ratio may need to be increased to get the higher *Ma* in order to improve the atomization. However, due to the energy loss increases accordingly, the customization and optimization of the atomizing nozzles become necessary.

Reference

[1] S.J. Martin, V.E. Granstaff, G.C. Frye, Characterization of a quartz crystal microbalance with simultaneous mass and liquid loading, Anal. Chem. 63 (1991) 2272–2281.
[2] S. Belfroid, W. Schiferli, G. Alberts, C.A.M. Veeken, E. Biezen, Predicting onset and dynamic behaviour of liquid loading gas wells, in: SPE Annual Technical Conference and Exhibition, Denver, Colorado, USA, 2008.
[3] N. Dousi, C.A.M. Veeken, P.K. Currie, Modelling the gas well liquid loading process, Society of Petroleum Engineers, United Kingdom, Sep. 6–9, 2005. Paper SPE 95282.
[4] S. Badie, C.P. Hale, C.J. Lawrence, G.F. Hewitt, Pressure gradient and holdup in horizontal two-phase gas-liquid flows with low liquid loading, Int. J. Multiph. Flow 26 (2000) 1525–1543.
[5] J. Yang, V. Jovancicevic, S. Ramachandran, Foam for gas well deliquification, Colloids Surf. A 309 (2007) 177–181.
[6] J.F. Lea, H.V. Nickens, M. Wells, Gas Well Deliquification, Gulf Professional Publishing, 2011.
[7] J.F. Lea, H.V. Nickens, Solving gas-Well Liquid-Loading Problems, vol. 56, Society of Petroleum Engineers, 2004, pp. 30–36.
[8] C.A.M. Veeken, S.P.C. Belfroid, New perspective on gas-well liquid loading and unloading, vol. 26, Society of Petroleum Engineers, 2011, pp. 343–356.
[9] M. Brandt, K.O. Gugel, C. Hassa, Experimental investigation of the liquid fuel evaporation in a premix duct for lean premixed and prevaporized combustion, J. Eng. Gas Turbines Power 119 (1997) 815–821.
[10] R. Sachdeva, D.R. Doty, Z. Schmidt, Performance of electric submersible pumps in gassy wells, Soc. Petrol. Eng. 9 (1994) 145–182.
[11] J.F. Lea, H.V. Nickens, M.R. Wells, Use of foam to deliquify gas wells, second ed., Gas Well Deliquification, Gulf Professional Publishing, Burlington, 2008, pp. 193–240.
[12] X.K. Li, Y. Xiong, D.J. Chen, C.J. Zou, Utilization of nanoparticle-stabilized foam for gas well deliquification, Colloids Surf. A 482 (2015) 378–385.
[13] Z. Schmidt, Nozzle-venturi gas lift flow control device and method for improving production rate, lift efficiency, and stability of gas lift wells, US5707214 A, 1998.
[14] A. Liknes, Method and apparatus for removing water from well-bore of gas wells to permit efficient production of gas, US20020007953 A1, 2002.
[15] H. Li, Z.L. Li, Digital simulation research on the downhole atomized nozzle for dewatering gas recovery, China Petrol. Mach. 08 (2009) 23–25.
[16] D.J. Harris, L.T. Wisniewski, A. Arian, R.B. Jones, G.L. Varsamis, Patent: acoustic artificial lift system for gas production well deliquification, US20140262229, 2014.
[17] L.L. Levitan, V.V. Salygin, V.D. Yurchenko, Method and apparatus for withdrawal of liquid phase from wellbore, US6059040 A, 2000.
[18] O. Shoham, Mechanistic Modeling of Gas-Liquid Two-Phase Flow in Pipes, Society of Petroleum Engineers, 2006, ISBN: 978-1-55563-107-9.
[19] R.G. Turner, M.G. Hubbard, A.E. Dukler, Analysis and prediction of minimum flow rate for the continuous removal of liquids from gas wells, J. Petrol. Technol. 21 (1969) 1475–1482.
[20] K.Y. Kim, W.R. Marshall, Drop-size distributions from pneumatic atomizers, J. Am. Inst. Chem. Eng. 17 (1971) 575–584.
[21] A.A. Rizkalla, A.H. Lefebvre, The influence of air and liquid properties on airblast atomization, J. Fluids Eng. 97 (1975) 316–320.
[22] G.E. Lorenzetto, A.H. Lefebvre, Measurements of drop size on a plain-jet airblast atomizer, J. Am. Inst. Aeronaut. Astronaut. 15 (1977) 1006–1010.
[23] N.K. Rizk, A.H. Lefebvre, Spray characteristics of plain-jet airblast atomizers, J. Eng. Gas Turbines Power 106 (1984) 175–180.
[24] ANSYS FLUENT 12.0 User's Guide, Ansys Inc, Evanston, IL, 60201.
[25] B.K. Park, J.S. Lee, K.D. Kihm, Comparative study of twin-fluid atomization using sonic or supersonic gas jets, Atomization Sprays 6 (1996) 285–304.
[26] J.F. Lea, H.V. Nickens, M.R. Wells, Gas Well Deliquification, second ed., Gulf Professional Publishing, Burlington, MA, 2008.